Mathematical Geology, Vol. 36, No. 1, January 2004 (© 2004)

Describing the Geometry of 3D Fracture Systems by Correcting for Linear Sampling Bias[1]

Olivier Fouché[2] and Jean Diebolt[3]

Analyzing the geometric bias inherent to linear sampling of natural fracture systems is a prerequisite to any attempt of structural modeling. In this paper, the basic parameters of 1D-sampled fracture sets, i.e. orientation, density, and size, are interpreted in terms of geometric probabilities. Weighting factors are derived which allow the 3D restitution of a moderately variable fracture network from a single borehole. The proposed method is applied to well core data from a granitic rock mass, and the efficiency of the proposed corrections is illustrated through random disc simulations tested by virtual scanlines analogous to the real borehole. This approach aims to reduce the prospecting effort in exploration, and to criticize assumption of structural homogeneity by rigorously comparing fracture populations collected from nonparallel boreholes. Then a parametric study of fracture size is performed and a range of mean size leading to fully connected networks is identified.

KEY WORDS: discontinuity, homogeneity, connectivity, anisotropy, stereology, stochastic process.

INTRODUCTION

Modeling the architecture of geological formations, *i.e.* their fracture arrangement and hierarchy, has been a foreground task for some 20 years in various disciplines, especially in hydrogeology (Black, 1994; Renshaw, 1998) and geomechanics (Meyer, Einstein, and Ivanova, 1999). Indeed the fluid flow, rock strength), and progressive deformation of rock masses are strongly affected by the connectivity and anisotropy of the fracture network (Berkowitz, 1995; Berkowitz and Adler, 1998). These two complex geometric features are not measurable in a real fractured medium; but they are derivable from topological analysis of a 3D artificial network mimicking the real one (Halbwachs and others, 1996). Thus,

[1]Received 17 July 2001; accepted 30 July 2003.

[2]LCPC (Central Laboratory of Bridges and Roads), Department MSRGI (Soil and Rock Mechanics & Engineering Geology), 58 Bd Lefèbvre, 75732 Paris cedex 15, France; e-mail: fouche@lcpc.fr or nfouche@ehess.fr

[3]Laboratoire Analyse et Mathématiques appliquées (Analysis & Applied Mathematics Lab.), CNRS, Université Marne-la-Vallée, 5 Bd Descartes, 77454 Champs-^{s}/Marne cedex 2, France; e-mail: diebolt@math.univ-mlv.fr

they result from the manner in which basic parameters (fracture orientations, sizes, and densities) have been inferred from field data and integrated in a chosen model (Baecher, 1983).

Boring deep holes in order to investigate rock masses below the first decameters is becoming more and more common in engineering practice, especially in civil and mining projects. Due to the high cost of drilling (among other reasons), it is often necessary for geologists to explore means of estimating fracture statistics based on borehole-censored data collected in only one or two directions (Barnes and others, 1997). The probability of cutting fractures within a small orientation range by a borehole depends on the following geometric factors: the fracture orientations, their shapes and sizes, and their abundance and positions in the volume of the explored rock mass, with regard to the borehole orientation, dimensions (length and diameter), and emplacement. For a given spatial arrangement of fractures, the sampling probability is lower for a set lying at a closer angle with the borehole axis, and characterized by less extended fractures or/and lower density. Thus, the image of the fracture network is complexly biased. Moreover, borehole data supply good orientation data but are very poor in their potential to inform about the fracture size values and distribution.

The main purpose of the present paper is to provide usable analytical formulas to correct borehole-sampling biases when estimating the basic parameters of a stochastic 3D fracture network in a lithologically homogeneous rock mass.

PROBLEMATIC AND METHODOLOGY

Knowledge of fracturing as a function of scale is critical to many geological pursuits, including the estimation of groundwater flow in the low-permeability rock masses that are candidates for the disposal of nuclear fuel wastes (Fouché and Lacquement, 2001). As part of long-term radioactive waste management, the feasibility of creating an underground research laboratory in a granitoïd pluton overlain by a 150-m thick sedimentary cover has been studied in France (Lebon and Mouroux, 1999). Preliminary field studies within a 225 km^2 area referred to as the Charroux–Civray Massif, including geophysical measures and description of cores from 15 deep boreholes and analogous outcropping rocks, have suggested that the structure of the intrusion is sufficiently consistent in character to be statistically treatable (Gros and Genter, 1997). The regional structural setting is favorable to an assumption of homogeneity. The rock volume under study is 500 m in depth and 500 m $\times$ 500 m in area. At this scale it is considered as lithologically homogeneous and it is not intersected by any first- or second-order weakness zone as defined in Pusch (1998). In the selected site, the only in situ available structural data were systematically collected from the drill cores of two nonparallel holes: Cha112 (vertical) and Cha212 (plunging 60°), respectively, 580- and 1000-m long. For the

first one, accounting for fractures conceivably sized between 1 m and 100 m, the partition of the fracture population into orientation sets is stable with increasing depth. Besides, the fracture frequency (i.e. number of fractures intersected per unit length along the borehole) describes a sinusoidal curve around a stable mean value (Fouché, 1999), with roughly a 100-m half-period. Therefore, based on fracture frequency, the fracture network cannot be viewed as strictly homogeneous with respect to depth at the 500-m scale. The same situation has been observed in the second borehole but due to geometric biases inherent to 1D sampling, we cannot directly infer that the mean orientation and 3D density of fracture sets (see section Density Bias Correction for a precise definition) are the same in the two boreholes. Actually, at this stage such a comparison is not straightforward. The existence of regular cycles of fracture frequency in both boreholes only suggests that the whole rock volume belongs to a global magmatic layering (Fouché and Meilliez, submitted). Since we are mainly concerned with the structural homogeneity at the 500-m scale, it is of primary importance to first correct sampling biases when performing the statistical analysis of the borehole-sampled fracture population.

Our paper reports a methodology that we have developed to estimate the basic geometric parameters relevant to the modeling of the in situ 3D fracture network, with the limited help of a single borehole. The second borehole has only been used as a reference to check the constructed model and discuss the homogeneity of the real fracture network. In this paper, we do not intend to report the full study of a natural site. Rather, our goal is to derive new simple analytical relations between sample data and the parameters of a fracture network model.

The problem is treated through a conceptual model, where the fracture network is simplified as the superposition of independent sets of random discontinuities (discs) in space. In this conception, each set expresses both the orientation variability and the irregularity of fracture surfaces. Our approach shortcuts the Monte Carlo procedures that are generally used to tune parameters until the model approximately matches the data. Here, we present in a first step how the orientation of average plane of each biased set can be adequately corrected from the orientation bias. The second step consists in evaluating the 3D density of each fracture set through an extrapolation based on the total fracture area measured within the volume of cores. Finally, a stereological estimate of the density bias allows us to propose a size hierarchy between the sets.

In order to check that our method of analysis actually yields accurate estimates of the population parameters, we have run virtual scanlines through stochastic simulations to provide a statistical sample of the possible outcomes. The indetermination of fracture size (disc diameter in the model) appears as a handicap and requires a parametric study through the model in order to examine the influence of the mean radius on the connectivity of the network (Bour and Davy, 1998).

ORIENTATION BIAS CORRECTION

The possibility of correcting geometric biases involves the existence of some organization of the fracture orientation data. Identifying sets in a sample of fractures requires the choice of 1. a grouping criterion of units (poles or dip-vectors), 2. a rule to assign each unit to a set, 3. an optimal number of clusters to part the whole population, 4. an orientation probability distribution of units within each set, and 5. a weighting inverse procedure able to restore the in situ relative attitude of the sets. The first three points and the fourth one may appeal respectively to a variety of algorithms in contouring or cluster analysis and to different model distributions, respecting as much as possible the degrees of uniformity, isotropy, symmetry, or multimodality of the actual population. Here, these four points will not be discussed. The first section of this paper is focused on the fifth point.

Studies on the borehole orientation bias (Priest, 1985; Wathugala, Kulatilake, and Stephansson, 1990) almost entirely rely on Terzaghi's method (1965), which first gave special attention to this problem through an inverse approach. Mauldon and Mauldon (1997) addressed the problem for circular fractures intersected by a sampling cylinder infinitely long in relation to its diameter, so that end effects could be ignored. They derived a correction factor as a function of the ratio between the cylinder radius and the fracture radius and showed that Terzaghi's correction reduces to the special case of a zero ratio, i.e. when the cylinder is a scanline or a borehole with negligible radius. Lately, the problem has been treated alternatively by a forward approach in the particular case of the borehole-biased uniform distribution, i.e. without identifying sets (Martel, 1999). In the present section, we aim to improve Terzaghi's method which has generally been used until now despite some deficiencies.

First Approximation of the Orientation Weighting

The borehole (scanline) orientation bias basically leads to underestimate the number of fractures of a specified orientation within the explored volume of the rock mass. The technique proposed by Terzaghi (1965) to correct this bias consists of a weighted counting polar diagram (Fig. 1(A). Poles of the fracture planes sampled from one borehole are plotted on an hemispherical net with isogonic lines drawn around the borehole axial point, θ denoting the angle between a fracture pole and the borehole axis. For each counting cell, lying in a field between two adjacent isogonic lines, she computes the ratio of the measured number of poles in the cell to the average $\cos\theta$ in this field. This corrected frequency is an estimation of the number of fractures which would be orthogonally intersected by a diameter of the unit sphere going through the cell, the unit being the length of the borehole. It is implicitly admitted that fractures are parallel and define a constant spacing within each cell. This correction produces a synthetic population which is larger

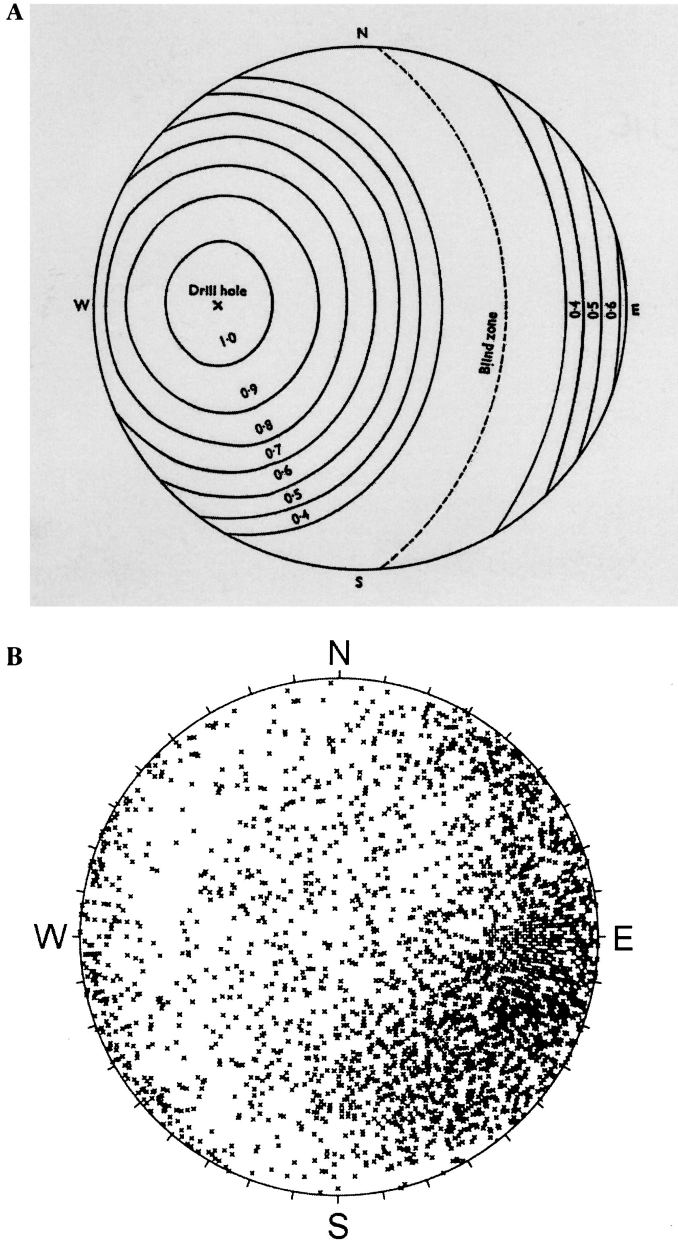

Figure 1. (A): isogonic lines for poles of fractures intersecting a borehole plunging 45° in stereographic projection; figures indicate approximate values of $\cos\theta$ for fractures represented by poles lying between same two lines, where θ denotes the acute angle between the pole-vector of the fracture and the borehole axis. (B): a fracture data set from borehole Cha212 (78;60): the blind zone clearly appears in the Wulff net.

than the sample and brings a more realistic image of the 3D overall orientation distribution. Following this operation, clusters are searched within the resultant augmented population. This method involves two basic difficulties:

First, in the field called "blind zone" according to the lack of data in the neighborhood of the blind 90°-isogonic circle (Fig. 1(B) for an example), the correction becomes unsecured since division by cosines close to zero leads to overestimate the real abundance of fractures in this particular orientation range. Therefore, grouping algorithms are likely to join together synthetic clusters lying on opposite sides of the blind isogonic circle. This may result in the paradoxical artifact of fracture sets with mean orientation strictly parallel to the borehole axis. In practice, this difficulty is often empirically dealt with by 1. neglecting the data within the "blind zone," whose range (commonly $\pm$ 20°) may be determined from the allowed weighting uncertainty and measurement accuracy, and 2. joining together several weighted counting diagrams associated with at least three variously oriented boreholes into a collective weighted counting diagram (Fig. 2). Nevertheless, if such data were available, one should carefully compare each sample with others before assuming structural homogeneity. Deservedly, orientation biases are often responsible for misleading conclusions when comparing samples from nonparallel boreholes.

The second weakness of Terzaghi's method is the choice of the cell size. The counting cell must be large enough for each one to enclose a subset with a sufficient number of poles. This is an implicit condition for the cosine correction to be applicable. However, this goes against a good resolution of the $\cos\theta$ fields. Moreover, the real fracture sets (if they exist) generally have not the same dispersion. Since they are still unknown at this stage of Terzaghi's method, any chosen cell size is hardly appropriate for all of them so that their subsequent identification may be altered.

We now attempt to solve these difficulties by clarifying the respective influences of orientation and frequency over the linear sampling probability, and showing that Terzaghi's correction is a limit weighting whose validity is restricted to samples with high number of fractures.

As a third weakness of Terzaghi's method, note that fractures are considered as persistent planes and that a possible correlation between orientation and size is not taken into account: mutual stochastic independence of orientation and size is implicitly assumed. We will briefly discuss this point.

Frequency-Dependent Orientation Weighting

To estimate the 1D sampling probability, it is helpful to consider an ideal fracture subset model consisting of parallel and equally spaced fractures (Fig. 3). Such an oversimplified model underlies Terzaghi's line of reasoning. This subset is intersected by a line OQ whose length L is measured between the first fracture and

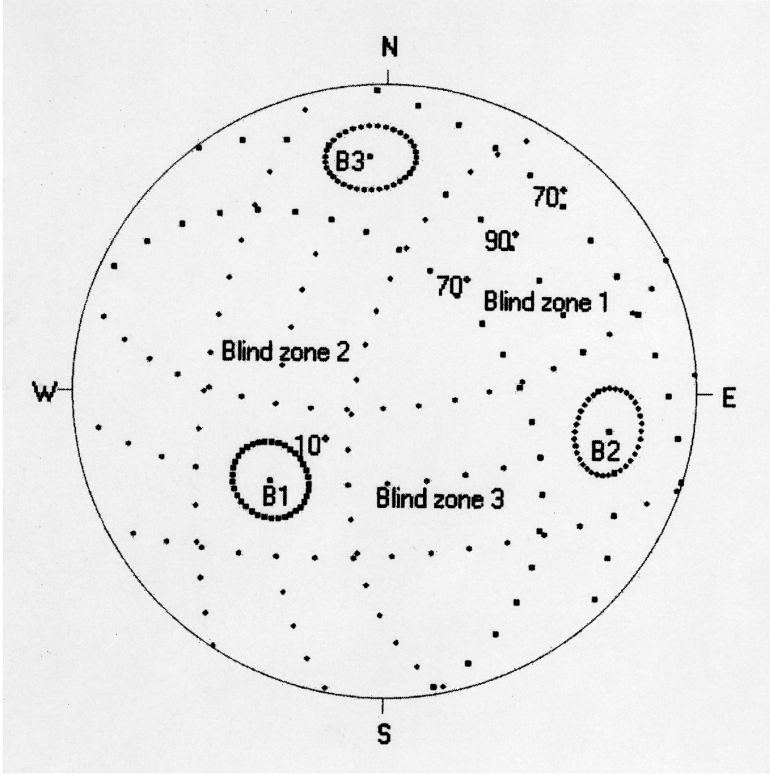

Figure 2. Blind zones associated to three orthogonal boreholes: B1, B2 and B3, each one represented by its axis surrounded with a 10° cone. The poles lying at 90° with borehole B1 are on a great circle containing the axes B2 and B3. This circle, which is referred to as the blind circle of B1, is depicted by a dotted line. The poles lying at an acute angle of 70° with B1 are on two circles, parallel to the blind one, that are also depicted. They bound the blind zone of B1. Idem for B2 and B3. The advantage of such an orthogonal system is the absence of overlap between the three blind zones together, and thus no region of the stereoplot is left with highly biased information.

the last one, thus providing an ideal sample of n parallel fractures. Let θ_o denote the acute angle between the common pole-vector of the subset and the borehole axis. Let N be the number of fractures of this set which would be orthogonally intersected by a line of the same length L. Our purpose is to express the sampling probability n/N as a function of n and θ_o.

Mean orthogonal spacing for a set may be defined as the mean distance between consecutive fractures that would be measured along a perpendicular scanline or equivalently, except for end effects, the length of this scanline divided by the number of fractures that would be intersected. Fracture frequency is

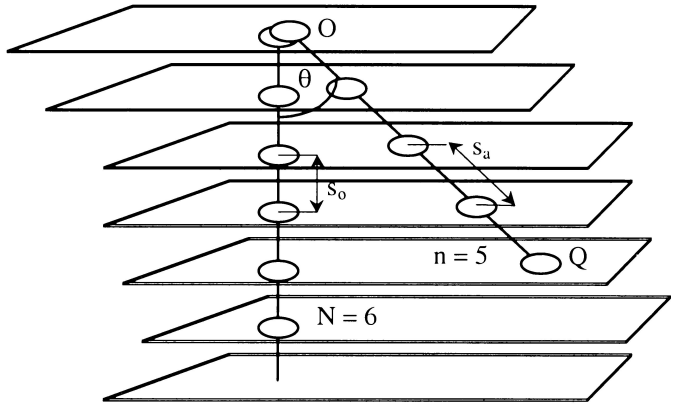

Figure 3. A subset of nearly parallel and regularly spaced fractures intersected by an oblique borehole and an orthogonal one, defining respectively the mean apparent spacing s_a and the mean orthogonal spacing s_o.

defined as the reciprocal of the mean spacing. In the above-described ideal subset the mean apparent spacing is $s_a = L/(n-1)$, and taking the end effect into account the mean orthogonal spacing s_o satisfies $L/N < s_o \leq L/(N-1)$ It follows that $(n-1)/N < s_o/S_a \leq (n-1)/(N-1)$, which can be split into the two following inequalities by using the relation $s_o = s_a \cdot \cos\theta_o$:

$$(n-1)/N < \cos\theta_o \quad \text{implying that} \quad (n-1)/\cos\theta_o < N$$

and $\quad \cos\theta_o \leq (n-1)/(N-1) \quad$ implying that $\quad N \leq 1 + (n-1)/\cos\theta_o$

Therefore, since N is an integer, we obtain $N = 1 + \langle (n-1)/\cos\theta_o |$, where $\langle K |$ denotes the largest integer $\leq K$, and the sampling probability for any subset of angle θ is

$$P_n(\theta) = \frac{n}{1 + \langle (n-1)/\cos\theta |} \tag{1}$$

The frequency-dependent weighting factor that we propose is

$$w_n(\theta) = 1/P_n(\theta) \tag{2}$$

Note that Equation (1) can be approximated by the limiting expression as $n \to \infty$

$$P(\theta) = \lim_{n\to\infty} \frac{n}{\langle n/\cos\theta |} = \cos\theta \tag{3}$$

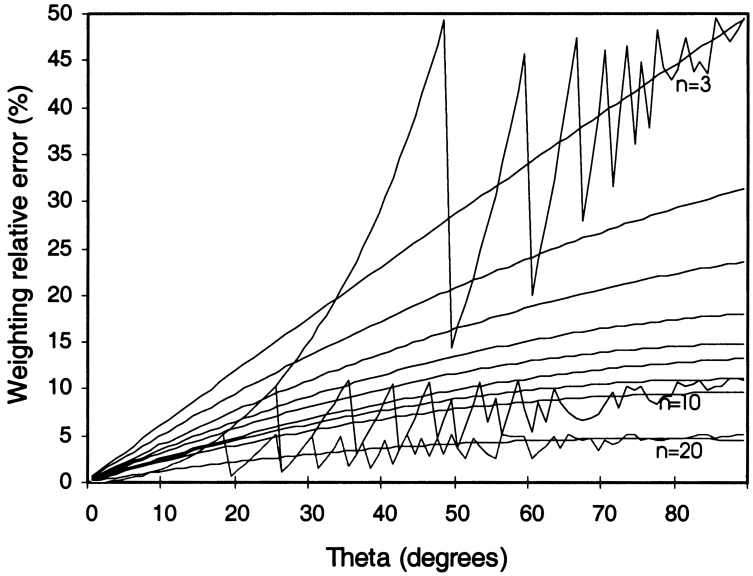

Figure 4. Second-order polynomial approximation of the relative error on bias correction as a function of n, number of fractures of the considered subset, and θ, acute angle between the pole-vector and the borehole axis.

When using the limiting weighting factor $w(\theta) = 1/P(\theta)$ known as Terzaghi's correction instead of Equation (2), the relative error is

$$\Delta w(\theta) = [w(\theta) - w_n(\theta)]/w_n(\theta) \tag{4}$$

For instance, assuming a measurement accuracy of 1 degree, the maximum value of the relative error is $\Delta w(89^\circ)$, reached for the poles close to the blind circle: as shown in Figure 4, for $n \geq 10$ this value is smaller than 10%, and with decreasing$n$ this maximum value rapidly increases (up to 100% for $n = 2$). Since 1. the number of data n is very small in a cell lying in the blind zone, and 2. Δw is not proportional to θ, it turns out that this error has a significant effect on a population of fractures. This emphasizes the advisability of a systematic frequency-dependent weighting of subsets.

If sets with a geological meaning actually exist, then their frontiers should remain clear within the whole biased distribution. When the data are grouped into clear-cut clusters, bias is likely to produce additional boundaries rather than suppress existing ones. Consequently, any bias-correcting procedure should 1. remove artificial boundaries, and 2. keep the true ones. We advocate that it is sensible to first determine clusters, and then apply corrections within each cluster

to expand it towards the blind circle. Doing that is more consistent than first increasing the number of points in the shadow zone of the stereoplot and then applying a cluster analysis.

The method we use to correct for mean orientation of a cluster identified as a fracture set is postponed till Appendix A. That method integrates a strong assumption of independence between azimuth and plunge which is needed to simultaneously correct for the density bias, as showed in the next section.

We have analyzed the underlying assumptions of Terzaghi's method and focused on the end effect. Whereas Terzaghi's method needs borehole data gathered in at least three directions to correct bias and finally identifies potential sets, we improve the procedure by first separating the biased clusters from only one borehole and then estimating their orientation parameters, accounting for the dispersion and frequency of each fracture set.

DENSITY BIAS CORRECTION

The spatial probability distribution of fractures within each set is the second basic attribute which contributes to the overall properties of a fracture network (Karcz and Dickman, 1979). It is represented by some measure of fracture density (Dershowitz and Herda, 1992; Mauldon, 1994), whose different definitions are recalled below. Relationships between them are analyzed in order to quantify the borehole density bias.

Definitions of Fracture Density

The measured 1D fracture frequency, i.e. the average number of intersected fractures per unit length, and the measured 2D fracture density, i.e. the average trace length per unit area, vary respectively with the orientation of the scanline or the sampling plane, except in the case of an isotropic fracture distribution. The measured 3D density of a given network, i.e. the average fracture area per unit rock volume, depends (as the measured 2D density does) on the relative dimensions of fractures and sampling regions.

In a region $\Re$ with volume V very large with respect to the areas a_j of the J fractures centered within $\Re$, the overall 3D density of the fracture network

$$A_V = \frac{1}{V} \cdot \sum_{j=1}^{J} a_j = d_3 \cdot \bar{a} \tag{5}$$

is determined from the bulk center intensity d_3 and the mean fracture area $\bar{a}$,

$$d_3 = J/V \tag{6}$$

and
$$\bar{a} = \frac{1}{J} \cdot \sum_{j=1}^{J} a_j \tag{7}$$

In the same way, in a plane region $\wp$ with area A cross-cutting I fractures in $\Re$, supposed to be very large with respect to the I trace lengths l_i centered within $\wp$, the overall 2D density of the trace network

$$L_A = \frac{1}{A} \cdot \sum_{i=1}^{I} l_i = d_2 \cdot \bar{l} \tag{8}$$

is determined from the area center intensity d_2 and the mean trace length $\bar{l}$,

$$d_2 = I/A \tag{9}$$

and
$$\bar{l} = \frac{1}{I} \cdot \sum_{i=1}^{I} l_i \tag{10}$$

The different density parameters have been studied with the tools of geometric probability theory and stereology (Santalo, 1976; Weibel, 1980). These studies have revealed fundamental relations which were found useful in the field of fracture network characterization and modeling when approximately isotropic uniform random scanlines or boreholes are available (Hudson and Priest, 1983; Rouleau and Gale, 1985). Here, we propose an approximate correction factor which allows us to estimate the 3D density of each fracture set from a single borehole.

Borehole-Measured 3D Density

Let us consider a cylindrical drill core of section $\pi\varepsilon^2$ (where the radius ε is less than 5 cm) and length L sampling n fractures. In practice, one rarely observes the boundary of a fracture within a core, and the condition $2\varepsilon/\cos\theta_i \leq E_i$, where E_i is the size of fracture i whose pole is at an acute angle θ_i with the core axis, is generally satisfied at the fracture scale considered for a repository for instance. We make the assumption (H) that each fracture i fully contributes to the 3D density measure. Under this assumption, the area of the portion of fracture i included in the rock cylinder is $\pi\varepsilon^2/\cos\theta_i$. Based on Equation (5), we estimate the borehole-measured 3D density under the assumption (H) indicated below by a tilde sign:

$$\tilde{A}_V = \frac{1}{L \cdot \pi\varepsilon^2} \cdot \sum_{j=1}^{n} \frac{\pi\varepsilon^2}{\cos\theta_j} = \frac{1}{L} \cdot \sum_{j=1}^{n} \frac{1}{\cos\theta_j} \tag{11}$$

We anticipate that assumption (H) leads to an overestimation of the 3D density (i.e. $\tilde{A}_V \geq A_V$) since it is independent of fracture size. We now show that this overestimation is systematic and controlled by a factor $F_n \leq 1$ such that, for each given set considered with stochastic independence of azimuth and plunge:

$$A_V \approx F_n \cdot \tilde{A}_V, \tag{12}$$

where

$$F_n = n^2 \Big/ \left(\sum_{j=1}^{n} \cos\theta_j \cdot \sum_{j=1}^{n} \frac{1}{\cos\theta_j} \right) \tag{13}$$

Borehole-Measured 2D Density

A population of J fractures of this set within a region $\Re$ is distributed into subsets of J_α fractures lying in a narrow range of azimuth δ_α around average azimuth α. For each subset, only one plane with azimuth α contains the borehole axis. In this plane, focus on a square region $\wp_\alpha$ of side L, where the borehole becomes the slot $[L/2 - \varepsilon \leq x \leq L/2 + \varepsilon;\ 0 \leq y \leq L]$ (Fig. 5). The fractures which intersect $\wp_\alpha$ produce I_α random segments (traces) of lengths $2r_i$ and average length $2\bar{r}_\alpha$ (computed from Eq. (10)), lying at angles θ_i with the Ox axis, with their centers $(x_i; y_i)$ in $\wp_\alpha$. Remark that the angle θ_i becomes the apparent plunge β_i in this special configuration. We assume that the random variables plunge, B, and semi-trace length, R, associated with probability density functions $f(\beta)$ and $g(r)$ respectively, are mutually independent, and that the horizontal distances between the centers and the borehole axis are a 1D Poisson process. The I_α traces and the n_α portions of these traces which are intersected by the slot allow us to calculate $(L_A)_\alpha$ and $(\tilde{L}_A)_\alpha$ respectively. In view of Equation (8) and according to assumption (H), the 2D density measured in the rectangular slot of length L and width $2\varepsilon \ll L$ is (note the similitude with Eq. (11))

$$(\tilde{L}_A)_\alpha = \frac{1}{2\varepsilon L} \cdot \sum_{i=1}^{n_\alpha} \frac{2\varepsilon}{\cos\beta_i} = \frac{1}{L} \cdot \sum_{i=1}^{n_\alpha} \frac{1}{\cos\beta_i} \tag{14}$$

From Equations (8) and (9) it results that

$$\frac{I_\alpha}{L^2} = \frac{(L_A)_\alpha}{2\bar{r}_\alpha} \tag{15}$$

In this 2D scheme, we wish to express the error made when estimating $(L_A)_\alpha$ by

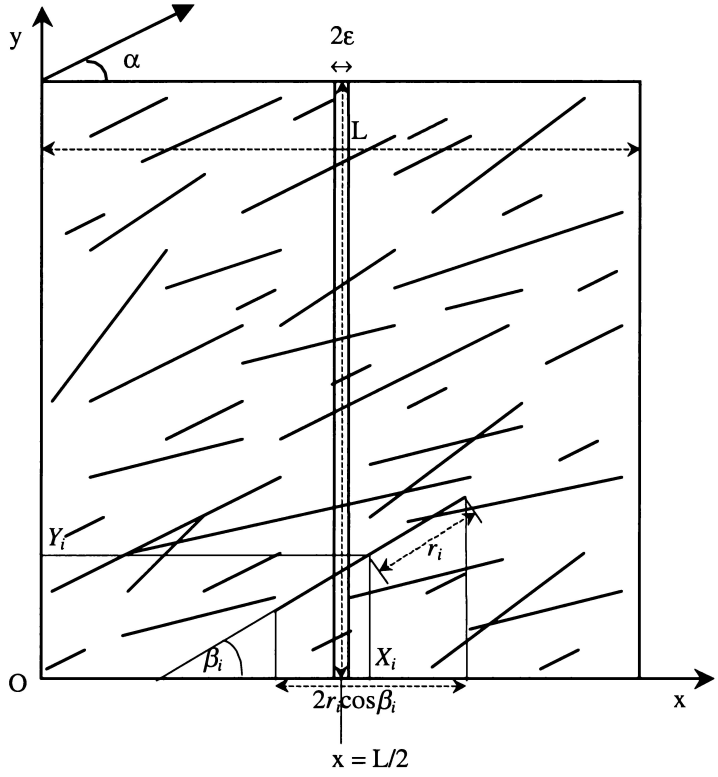

Figure 5. Intersection of traces of a fracture subset in a plane $\wp_\alpha$ by a 1D sampling slot. See the text in section Borehole-measured 2D density for comments.

$(\tilde{L}_A)_\alpha$, which from Equations (14) and (15) is equivalent to estimating I_α by

$$\tilde{I}_\alpha = \frac{L}{2\overline{r_\alpha}} \cdot \sum_{i=1}^{n_\alpha} \frac{1}{\cos\beta_i} \tag{16}$$

The remaining part of our proof is postponed until Appendix B. Finally, in view of Equation (16) and Equation (32) established in Appendix B, we find that $I_\alpha = F_\alpha \cdot \tilde{I}_\alpha$, where F_α is defined from Equation (13) by replacing n with n_α.

At this point, precise knowledge of the centers $(x_i; y_i)$ probability distribution is not necessary since the y_i are not involved in the proof. Moreover, the correction factor F_α remains roughly valid whenever the X_i's can be approximately considered as uniform random variables on the studied interval. Also, no assumption is needed concerning the form of the size probability distribution whereas the shape of the discontinuity surfaces (discs or other plane convex shapes) has not to be specified.

From 2D Density to 3D Density

Since azimuth and plunge of fractures are assumed to be independent within each set, the approximations proposed in Equations (30) and (31) (see Appendix B) lead to the approximation that the values taken by F_α are independent of α whenever n_α is large enough. Therefore, a better estimate of the common value of the F_α's is F_n given by Equation (13). Thus, we obtain $I_\alpha \approx F_n \cdot \tilde{I}_\alpha$, already noticed to be equivalent to

$$(L_A)_\alpha \approx F_n \cdot (\tilde{L}_A)_\alpha \tag{17}$$

According to Equations (11) and (14) and noting that $n = \sum_\alpha n_\alpha$, the summation $\sum_\alpha$ of Equation (17) on the whole range of α for the considered set provides

$$\sum_\alpha (L_A)_\alpha \approx F_n \cdot \sum_\alpha (\tilde{L}_A)_\alpha = F_n \cdot \tilde{A}_V \tag{18}$$

Finally, proving Equation (12) boils down to proving that

$$\sum_\alpha (L_A)_\alpha \approx A_V \tag{19}$$

Now, we have to assume an a priori model of disc-shaped fractures whose centers are an isotropic 3D Poisson process with intensity d_3 (defined in Eqs. (5) and (6)). Fracture size is represented by disc diameter D. We suppose that D is a random variable independent from azimuth and plunge. Under our conditions, and without assumption on the form of the diameter probability distribution, Warburton (1980) establishes that

$$(d_2)_\alpha = (d_3)_\alpha \cdot \mathbf{E}(D) \cdot \cos\gamma \tag{20}$$

and

$$\mathbf{E}(2R) = \frac{\pi}{4} \cdot \frac{\mathbf{E}(D^2)}{\mathbf{E}(D)}, \tag{21}$$

where $-\frac{\delta_\alpha}{2} < \gamma < +\frac{\delta_\alpha}{2}$ expresses the deviation of pole-vectors from the mean plane of $\wp_\alpha$. In our case where $\gamma \approx 0$, summation of Equation (20) leads to

$$\sum_\alpha (d_2)_\alpha \approx \mathbf{E}(D) \cdot \sum_\alpha (d_3)_\alpha \tag{22}$$

Equation (5) implies $(A_V)_\alpha = (d_3)_\alpha \cdot \bar{a}_\alpha$, where $\bar{a}_\alpha$ is computed from Equation (7) by replacing J with J_α. It follows from the mutual independence of D and α and

the A-E approximation (defined in Appendix B) that

$$A_V = \sum_{\alpha} (A_V)_\alpha \approx \mathbf{E}(\pi (D/2)^2) \cdot \sum_{\alpha} (d_3)_\alpha \tag{23}$$

Equation (8) implies that $(L_A)_\alpha = (d_2)_\alpha \cdot 2\bar{r}_\alpha$. Since the spatial distribution of the discs is isotropic, the expectation of trace length conditioned by α is independent from α and it follows from the A-E approximation that

$$\sum_{\alpha} (L_A)_\alpha \approx \mathbf{E}(2R) \cdot \sum_{\alpha} (d_2)_\alpha \tag{24}$$

Equations (22) and (24) together imply that

$$\sum_{\alpha} (L_A)_\alpha \approx \mathbf{E}(2R) \cdot \mathbf{E}(D) \cdot \sum_{\alpha} (d_3)_\alpha \tag{25}$$

From Equations (23) and (25) it follows that

$$\sum_{\alpha} (L_A)_\alpha \approx A_V \cdot \frac{\mathbf{E}(2R) \cdot E(D)}{\mathbf{E}(D^2 \cdot \pi/4)} \tag{26}$$

Finally, we conclude from Equations (21) and (26) that Equation (19) is established. Let us underline that Equation (12) is a rough approximation since it heavily relies on both the mutual independence of azimuth, plunge, and size, and the A-E approximation (see Appendix B) which means applying the law of large numbers to limited samples. Nevertheless, the correction factor F_n is likely to provide a good estimate of the 3D density only depending on orientations and frequencies measured in one borehole.

DENSITY BIAS, DISPERSION, AND SIZE

We now wish to gain some insight into the mean fracture size and reduce the vagueness on this third basic parameter. A fundamental relation of stereology states that an estimate of the 3D global density A_V is twice the average linear frequency $\bar{N}_L$ measured in a large array of isotropic uniform random scanlines. For one fracture set of known A_V the borehole frequency bias is expressed as the ratio b_θ increasing with θ:

$$b_\theta = (N_{\mathrm{L}_\theta} - \bar{N}_{\mathrm{L}})/\bar{N}_{\mathrm{L}} = (2 \cdot N_{\mathrm{L}_\theta} - A_V)/A_V \tag{27}$$

Table 1. Comparison Mode of Two Sets S and T

	If $\sigma_T < \sigma_S$	If $\sigma_T \approx \sigma_S$	If $\sigma_T > \sigma_S$
And $\delta_T < \delta_S$	$E_T \approx E_S$	$E_T > E_S$	$E_T \ll E_S$
And $\delta_T \approx \delta_S$	$E_T < E_S$	$E_T \approx E_S$	$E_T > E_S$
And $\delta_T > \delta_S$	$E_T \ll E_S$	$E_T < E_S$	$E_T \approx E_S$

When N_{L_θ} coincides with $\bar{N}_{\mathrm{L}}$, there is no bias and $b_\theta = 0$. The bias is positive if $N_{\mathrm{L}_\theta} > \bar{N}_{\mathrm{L}}$ (overestimation of frequency) and negative in the other case (underestimation of frequency).

Let us consider, as a reference model for a fracture set, a series of parallel infinite planes, whose mean normal vector makes an angle θ with the borehole axis. In this model, Equations (6) and (8) lead to $A_V = \tilde{A}_V = N_{\mathrm{L}_\theta}/\cos\theta$ and the bias is

$$b(\theta) = N_{\mathrm{L}_\theta} \cdot \left(2 - \frac{1}{\cos\theta}\right) \cdot \frac{\cos\theta}{N_{\mathrm{L}_\theta}} = 2\cos\theta - 1 \tag{28}$$

If one uses $b(\theta)$ as an approximation to b_θ (defined in Eq. (27)) for each set, the gap between the real fracture distribution and its equivalent parallel infinite model is characterized by $\delta(\theta) = |b(\theta) - b_\theta|$. Then we can class the sets according to this gap. Comparing the sets by pairs and accounting for their parallelism default (each set having known dispersion σ), one can deduce from δ some semiquantitative arguments on their relative mean sizes. This comparison method of two sets S and T is summarized in Table 1. For instance, considering two sets with the same dispersion (see column 2 of Table 1), a lower δ would imply a higher size. In the case of a pair having the same δ (see line 2 of Table 1), for the two sets to display the same gap with the parallel infinite model, a lower dispersion should be compensated by a lower size.

ILLUSTRATION IN A STOCHASTIC MODEL

Our methodology was applied to a fault population sampled from the two boreholes implanted in a selected site, part from the Charroux–Civray granite massif already mentioned in the Problematic and Methodology section. The number of sets, requiring independent characterization to create the network, was determined by analyzing the core data on faults (i.e. fractures that exhibit indicators of shear) with both visual inspection of stereoplots and a grouping algorithm. The six-sets configuration obtained from the vertical borehole Cha112 is stable for 400 m in depth: is it the same configuration in both Cha112 and Cha212 after correcting

Table 2. Primary (P) and Weighted (W) Orientation Parameters of the Six Identified Sets

Number of fractures per set	Mean P-azimuth	Mean P-plunge	std deviation P-plunge	Mean W-plunge	std deviation W-plunge
1: 17	108	32.5	11.0	32.7	9.4
2: 74	248	63.2	17.7	75.7	23.5
3: 36	307	60.1	12.8	65.2	15.9
4: 57	166	54.1	13.4	57.8	14.4
5: 18	24	70.5	7.5	74.0	7.9
6: 34	107	74.4	7.9	81.0	10.9

for the orientation bias? The departure of our corrected mean orientation from the unweighted one was currently valued between 1° and 12° for each set of Cha112 (Table 2). This effect could be sufficient to explain the difference between the stereograms of the two boreholes (Figs. 1(B) and 6(A)). Our modeling approach aims to control the validity of our corrections and to question the homogeneity of the fault network between the two boreholes.

In order to generate a realistic network of discontinuities for a statistically homogeneous region of the site in question, we use the Boolean model of random flat discs described by Aler, Du Mouza, and Arnould (1996), which is adapted from the principles introduced by Baecher, Lanney, and Einstein (1977). One major advantage is its flexibility in terms of size (diameter) distribution.

Scale of Study and Process of Fault Position Within a Set

To be consistent with the assumptions on which our corrections are based, the distribution of orientations in each set was modeled by independent azimuth and plunge. Orientation of discs was generated from uniform or normal distributions calculated from observed dip azimuth and plunge (see Appendix A). Once the optimum selection of sets and their statistical parameters are obtained, the relevant modeling scale of the network of superposed sets is determined from the order of magnitude of both fault frequency and size.

Based on core and field observations of their morphology, three classes of fractures were distinguished and faults were characterized with an empirical relation between size and infill width (Fouché, Cojean, and Arnould, 2001). The size hierarchy obtained from this relation, mean half-size (disc radius) of the six fault sets taking values (Table 3) in the interval [3 m; 12 m], was discussed and confirmed with the help of the estimate $\delta(\theta)$ defined in the previous section. According to this estimated size range, the modeling scale should be at least 20–30 m. At the low level of information inherent to borehole data, fault size E may be modeled by a truncated negative-exponential distribution, whose parameter λ is simply related

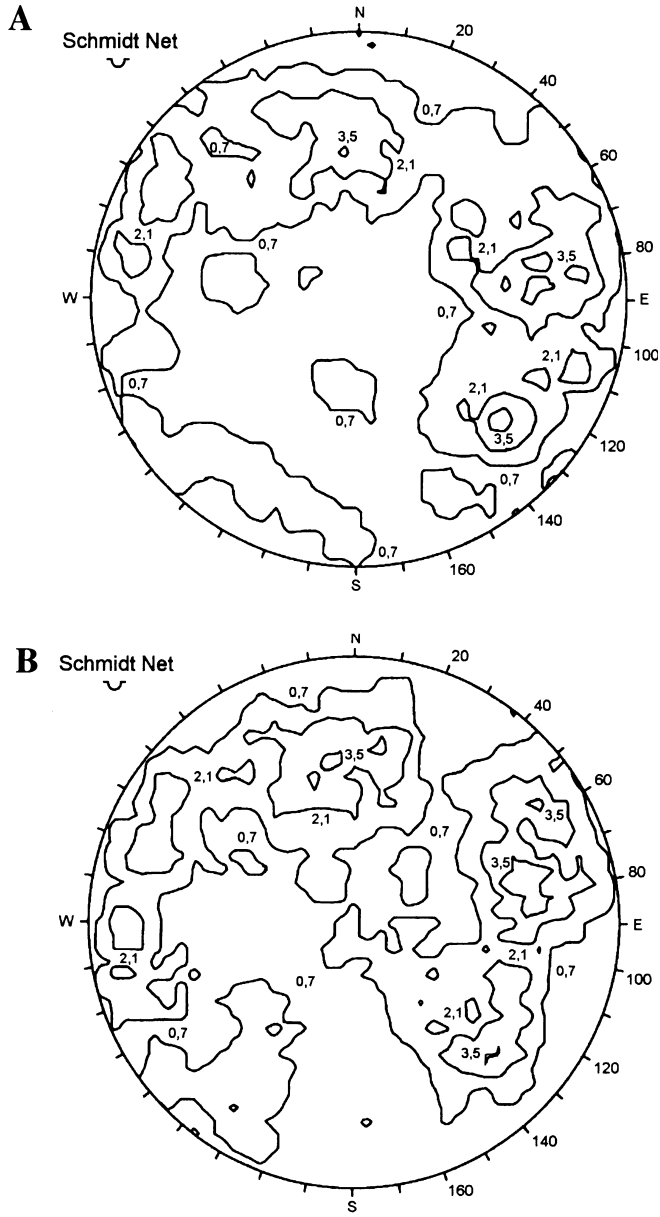

Figure 6. Visual comparison of actual borehole-sampled and virtual scanline-sampled distributions of fracture orientations: density contours in equal-area projection, with step = 1.4. (A): Poles of faults in the vertical borehole Cha112 (236 units, 260 m): Dimitrijevic counter: 2994 points. (B): Poles of discs in 26 vertical virtual scanlines of length 10 m (227 units, mean frequency = 0.87/m)—Six sets stochastic simulation within a cubic volume: Dimitrijevic counter: 2850 points.

Table 3. Primary and Corrected Density Parameters and Size of the Six Modified Sets

Number of fractures per set	Frequency N_L (/m)	3D density A_V (/m)	Correction factor F	Mean radius (m)	Intensity d_3 (10 m)$^{-3}$
1: 16	0.07	0.08	0.984	3.0	2.8
2: 50	0.21	0.82	0.573	11.5	1.1
3: 33	0.15	0.33	0.823	9.8	0.9
4: 46	0.20	0.41	0.804	8.5	1.5
5: 15	0.06	0.21	0.782	4.8	2.3
6: 29	0.12	0.62	0.668	10.7	1.2
Total: 189	Total: 0.81	Total: 2.47	—	Global: 9.1	Total: 9.7

to the mean value $\bar{E}$ and the minimum value E_m: $1/\lambda = \bar{E} - E_m$. Also, this choice makes it easier to analyze spacing and size relationships since we further choose the same type of distribution for spacing.

Decreasing the length of a gliding window from 100 to 10 m allowed us to determine the critical scale where second-order variations of fault frequency appear (here, 20 m), the main features remaining unchanged (Fouché, 1999). Consequently, we are interested in the fault network within local cubic boxes of typical edge size 20 m. A threshold Y_s of spacing values under which two consecutive faults are not distinguishable was specified as a percentage of the study scale (here $Y_s = 0.01 \times 20$ m $= 20$ cm). At this scale, we can treat closely spaced multiple-segment fractures as single units (Vermilye and Scholtz, 1995) by applying the spacing threshold and eliminating redundant data (this explains why the number of faults within each set is lower in Table 3 than in Table 2). Then, we observe that the spacing distribution is modified towards a negative-exponential model. This property has been assumed to hold for all other directions.

So, we focus on second-order variations of the fault frequency within each 20-m box where we can model the fault center distribution of a set by a stationary point process characterized by the local mean value of the 3D density. At this scale, based on stationarity and exponential distribution of spacing, it is reasonable to assume that the spatial distribution of disc centers within each set of the model is a 3D Poisson process of intensity d_3 (Eq. (5) and Table 3) combined with a representative sampling of fault orientations.

Verification and Comparison Through Stochastic Simulations

The efficiency of our corrections for orientation and density was confirmed by applying cluster analysis, hemispheric projection, and density measures to samples of virtual scanlines in the simulated regions. We aim to verify whether scanline samples from stochastic networks simulated with corrected parameters return the

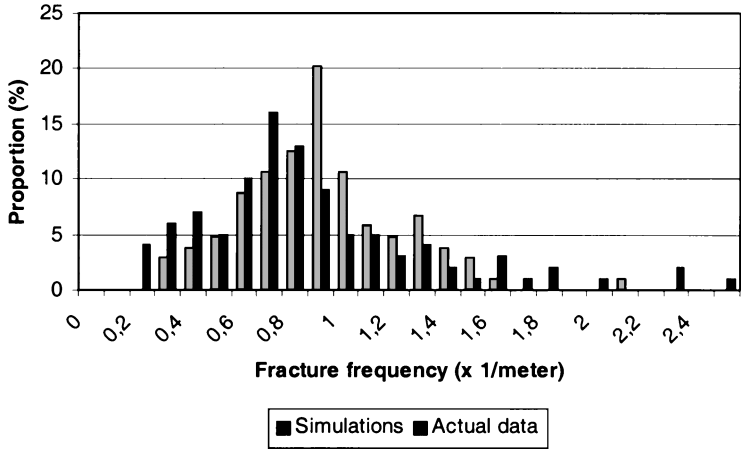

Figure 7. Histogram of measured and simulated frequencies in a 10-m gliding window (about 100 data). When the outliers are removed, this histogram is compatible with a rescaled 1D Poisson distribution which arises from a 3D Poisson point process. This argues in favor of modeling the fracture center distribution with a 3D Poisson point process. Outliers, or redundant fractures, are rather nuisances than proper data. We decided to remove it, which results in a better fitting of empirical and generated histograms with a same Poisson-type distribution.

same biased distributions as the real single borehole. The physical resemblance of the simulated geometry to that of the actual rock mass is one of the main criteria for assessing the degree of confidence in the results produced.

The virtual scanlines, when traced vertically, give samples very similar to the real vertical borehole Cha112 (Figs. 6(A) and 6(B)). This leads to the conclusion that we have produced the correct number of sub-vertical faults with the correct azimuths. The local variations of frequency are displayed in Figure 7 together with values of frequency from a series of 20-m long virtual scanlines through the 3D Poisson model. This empirical distribution indeed looks like a Poisson distribution of the same mean value, except for the influence of extreme data which moves the distribution to the left.

When traced obliquely, the virtual scanlines give samples similar to the real oblique borehole Cha212 except for two features: a 15° rotation of the overall distribution of poles appears in the stereoplot, and we observe that one of the six fault sets identified within the actual population of Cha112 (set n°4) still exists in the oblique virtual scanlines, despite the orientation bias, whereas it is not visible in Cha212 (Figs. 1(B) and 6(A)). Hence, the differences between the vertical borehole and the oblique one could not be reduced to an effect of the orientation bias through an homogeneous network. These divergences confirm that mixing the data of the two boreholes at the beginning of our modeling process would have meant an unjustified hypothesis of homogeneity.

Fault Size and Connectivity of the Network

Once the computer has simulated all the discs in space, the mutual intersections are examined through topological analysis. These intersections give rise to the formation of traces (intersection of at least two discs), vertices (intersection of at least three traces), edges (segment of a trace terminated at each end by vertices), and faces (a surface bounded by edges and vertices). These various elements are analyzed to determine the pathways and blocks that are possibly formed through the network. Parts of planes that do not contribute to isolate complete blocks are identified. The program then calculates the block volume distribution of all the completely formed blocks. A full discussion of this 3D modeling program can be found in Xu and Cojean (1990).

A parametric study of the influence of fault size (disc diameter) was performed in the case of 10-m long virtual scanlines, which represent the scale of a gallery for a possible underground laboratory. Each line of Table 4 displays results from a Monte Carlo simulation experiment with 26 replications for a given value of the mean radius of generated discs. The mean values and standard deviation have been obtained by averaging over the 26 replications. The first model scheme displays overestimated values of $N_{\mathrm{L}10}$ and A_{V10} because the ratio of minimum size to mean size $E_{\mathrm{m}}/\bar{E}$ becomes too large. Except for this case, the obtained values of $N_{\mathrm{L}10}$ and A_{V10} are the correct ones, i.e. the same as in the real borehole (compare with total values in Table 3). Note that our estimated mean fault size was about 18 m, which is close to the second model scheme. The results about the cubic root of the mean block volume illustrate the consistency of the model when the mean fault radius varies in the approximate range [5–30] m. These results suggest that: 1. The bias corrections are efficient, 2. The model is not sensible to the uncertainty on the mean radius since values of $\bar{E}/2$ are admissible in a large range. Moreover, in our

Table 4. Density Results of Stochastic Simulations for Several Values of Mean Radius (Half-Size): Mean Values and Standard Deviation (Indicated in Brackets)

Mean radius (m)	$N_{\mathrm{L}10}$ (/m)	A_{V10} (m^2/m^3)	*NI* discs	*NC* discs	Mean *BVD* (m)	Median *BVD* (m^3)
4.2	1.1 (0.3)	3.2 (1.4)	157 (10)	46 (6)	0.46 (0.05)	2.29 (0.71)
7.6	0.9 (0.3)	2.6 (1.1)	84 (9)	12 (2)	0.53 (0.07)	2.13 (0.79)
16.7	0.9 (0.3)	2.6 (1.2)	58 (9)	4 (2)	0.55 (0.11)	1.76 (0.41)
32.9	0.8 (0.4)	2.4 (1.0)	50 (8)	1 (1)	0.56 (0.12)	1.81 (0.49)

Note. $N_{\mathrm{L}10}$ is the fracture frequency measured in a 10-m virtual scanline. A_{V10} is the 3D fracture density measured in a 10-m virtual scanline. *NI* discs is the number of discs intersecting the simulation domain. *NC* discs is the number of discs centered within the simulation domain. Mean *BVD* is the cubic root of the mean value of the Block Volume Distribution. Median *BVD* is the median value of the Block Volume Distribution. Minimum radius = 0.5 m—Volume of the simulation domain = 1000 m^3 (cube of edge 10 m).

model, the number of discs that do not contribute to form blocks was systematically less than 5% of the total number of the discs intersecting the simulated network, whatever the mean radius in the range [5; 30] m. This result reveals that the network can be viewed as fully connected in a realistic range of fault sizes. Let us recall that this conclusion is supported by geological arguments, such as the ubiquity of calcite filling that crystallized throughout the fractured granite rock mass during a late water circulation event.

DISCUSSION

Here, our purpose is not to discuss different fracture network models (Chilès and de Marsily, 1993; Dershowitz and Einstein, 1988) from a realistic geological point of view.

Abundant literature, including our case study, provides evidence for the realism of a negative-exponential form for the spacing distribution of fractures along a scanline (Ferguson, 1985). The question of the size distribution of fractures in space is not tackled here although it is undoubtedly important (LaPointe and Hudson, 1985). Our choice of a negative-exponential form for this unknown parameter is plausible while we admit that it is somewhat arbitrary. Since geological evidence of a simple relation between fracture size and spacing exists, the regular spacing condition introduced in the section named Frequency-dependent orientation weighting (Fig. 3) may be satisfied if each iso-orientation subset is separated into approximately iso-size subsets. Whereas this "disaggregate characterization" (Gillespie and others, 1993) would lead to subsets with few data, the commonly implicit use of the law of large numbers in correcting for the orientation bias is a source of error which we have estimated and proved significant.

We do not try to model each orientation cluster with some parametric family of distributions. Instead, we only describe a cluster in terms of its two first empirical moments. The bias-correction only concerns the first moment of each cluster and we also provide an approximate corrected value of empirical dispersion. Therefore, we do not have to fit orientation distributions based on censored populations. Actually, testing the goodness-of-fit of various distribution families (Fisher, Bingham, etc.) on clusters of data is tedious and often fails (Kulatilake, Wathugala, and Stephansson, 1993; Starzec and Andersson, 2002). The only basic assumption that we make is the independence of α and β within each set: this corresponds to a nonparametric approach which keeps open a large range of flexible distribution forms. The robustness of the latter hypothesis could be further studied through Monte Carlo numerical simulations.

Otherwise, a radically different alternative approach would be to estimate the parameters of a mixture of distributions from some parametric family (with unknown number of components) based on censored data in a general missing data

framework, using the Expectation Maximization algorithm. But this is the subject of a forthcoming paper.

We have assumed that within each set the random variable θ can be parted into two independent variables α and β. Considering the overall distribution of orientation as a finite mixture of distributions, this assumption means that each component distribution is the product of a distribution on α and a distribution on β. Such an assumption is obviously not rotationally invariant and does not reflect the genesis of fracture sets (Marrett, 1996). Mechanical intuition indeed suggests that initiation and propagation of fractures over time lead to interdependent fractures (and even interdependent sets). Our assumption should rather be understood as part of our modeling approach, which requires simplifications and approximations. Such an assumption lies at the same simplification level as assuming that the point process of the centers is Poisson, or that the fracture network is a superposition of independent sets of random discontinuities. Besides, when looking at the (α, β)'s within each set in our case study (Fouché, 1999), it turns out that our independence assumption cannot be clearly rejected. Actually, the modulus of the correlation between α and β never exceeds 0.4 and is often much smaller.

We are conscious that fracture size could be significantly correlated with orientation within each set. In such a case, we would have to replace $f(b) \cdot g(r)$ with $f(b) \cdot g(r|b)$ in Equation (28 bis), where $g(r|b)$ denotes the conditional probability density function of R (size r) given B (plunge β). Intricate mathematical derivations could then be pursued and numerical computations could be made. However, it is impossible to conjecture what $g(r|b)$ should be, based on borehole sampling: we would face a typical ill-posed problem. Moreover, we have some reasons to suspect that R and B are approximately independent within each set: 1. Based on the natural assumption that fracture size and width are correlated (Vermilye and Scholtz, 1995), we can expect that the existence of a correlation between size and orientation would entail correlation between width and orientation. But the latter is not supported by available data (Fouché, 1999). 2. The outcomes of simulations and confrontation with the data issued from the second borehole seem to confirm the validity of our bias-correction formulas. It is worth noting that whereas we assume independence of size and orientation within each set, the superposition of several independent sets having different mean fracture sizes results in a strong dependence structure between size and orientation throughout the whole network.

Examining what situations tend to make an ordinary fracture a conductive one, we envisage the two following ones: large fractures have higher probability of intersecting other fractures and fractures that have experienced some shear probably have enhanced permeability. The indetermination of fracture size, which appeared as a handicap at the beginning of the study, has been shown to be of minor influence on the connectivity as far as the ratio of mean radius to minimum radius is large enough.

We only have shown the results of simulations for the regions of the borehole where the mean values of frequency and density prevail. In other regions of the borehole, the local mean frequency is lower and thus the network could be no longer fully connected. In those regions, the connectivity study would require more precise characterizations. Hence, the study of the network connectivity has to be further pursued.

The proposed model including bias corrections is robust with respect to the mean fracture size when disc radius is modeled as a truncated negative exponential distribution. Further robustness studies are recommended in order to test the sensibility of the model to the type of size distribution, the ratio of mean radius to minimum radius, and the assumption of independence of azimuth and plunge of dip vector.

CONCLUSIONS

In this paper, an improved output from 1D sampling through fracture networks is provided by introducing three complementary tools based on the probabilistic nature of finite fracture sets. Underlying is the ignorance of the fracture size or even the trace length distribution. In the view of a model conditioned by measured information (Andersson, Shapiro, and Bear, 1984), these tools based on simplifying assumptions only depend on the orientation-related frequency of the fractures observed in one borehole.

First, we have revisited Terzaghi's correction for the orientation bias. Some difficulties encountered with this classical method in the identification of directional sets from borehole data and in the discussion of homogeneity have been solved by formulating a frequency-dependent weighting applied to nearly parallel fracture subsets with necessary a quite regular spacing. Our formulas allow us to make a more reliable estimate of the mean value of fracture set dip.

Second, a correction factor of 2D density has been generalized by explicitly appealing to the law of large numbers, under the assumptions that the borehole diameter is negligible in comparison to trace lengths, and that azimuths and plunges of fractures are independent random variables. Then, assuming that fractures are disc-shaped and their positions follow an isotropic 3D Poisson process, the correction factor has been extrapolated to 3D, remembering stereology results. In this a priori model, anisotropy only results from the relative attitude of the sets.

Third, a major deficiency of current methods is their inability to analyze spatial distributions in relation to fracture sizes. Here, the departure of each identified set from a parallel infinite planes model has been quantified by a factor based on a stereological estimate. Comparison between the sets with regards to dispersion and size serves to control the hierarchy of mean size values estimated from the width of the infill material. This half-quantitative approach of size would be the

basis for a study of the specific influence of each set on the connectivity of the whole network.

It is possible to draw the following conclusions based on the results of validation attempts.

The proposed corrections are applicable to fracture networks regular enough at a specified scale to be modeled by a Poisson process. Their validity has been briefly illustrated through stochastic simulation and testing on a real example relative to a granitic rock mass. These corrections result in a cumulated influence on anisotropy and connectivity of the network. They allow to discuss the homogeneity of the geological structure in the region between two boreholes, here at the 500-m scale. The considered population of fractures, of metric to pluri-decametric order in size, can play the role of low conductivity connection between the hectometer-order faults which are present in the studied rock mass.

Our methodology was initially applied to natural fractures and directed towards rock engineering problems, especially to avoid abusive and unwarranted amalgamation of biased data, and to reduce the prospecting effort in geological exploration through well boring. We expect that it will turn out to be useful in the fundamental fields of structural geology and petrology, textural mineralogy, or geomorphology. As a perspective, we intend to apply our methodology to sets of cracks produced in a rock sample under controlled mechanical loading (Fouché and others, in press) in order to gain in our understanding of deformation and percolation in the excavation-disturbed zone around a laboratory for long-term testing of nuclear waste storage.

ACKNOWLEDGMENTS

This work was carried out within the framework of a cooperation between the French Agency for Radioactive Waste Management (ANDRA) and the Engineering Geology Center (CGI) which is common to the National School of Mines of Paris (EMP) and the National School of Bridges and Roads (ENPC). Particular thanks are due to W. S. Dershowitz and an anonymous reviewer for critical remarks and constructive comments.

REFERENCES

Aler, J., Du Mouza, J., and Arnould, M., 1996, Measurement of the fragmentation efficiency of rock mass blasting and its mining applications: Int. J. Rock Mech. Min. Sci. Geomech. Abstr., v. 33, no. 2, p. 125–139.

Andersson, J., Shapiro, A. M., and Bear, J., 1984, A stochastic model of a fractured rock conditioned by measured information: Water Resour. Res., v. 20, no. 1, p. 79–88.

Baecher, G. B., 1983, Statistical analysis of rock mass fracturing: Math. Geol., v. 15, no. 2, p. 329–348.

Baecher, G. B., Lanney, N. A., and Einstein, H. H., 1977, Statistical description of rock properties and sampling, *in* Proceedings of the 18th US Symposium on Rock Mechanics, Colorado School of Mines, Golden: American Institute of Mining Engineers, New York, pp. 5C1.1–5C1.8.

Barnes, R. P., Bowden, R. A., Dee, S. J., Cavill, J. E., and Kingdon, A., 1997, A structural atlas of discontinuity data from Nirex deep boreholes at Sellafield, UK—Interpretation of structural domains and compensation for borehole orientation censoring, *in* Proceedings of the 9th Symposium of the European Union of Geosciences, 23–27 march 1997, Strasbourg, France: Abstract supplement to Terra Nova, v. 9, p. 297.

Berkowitz, B., 1995, Analysis of fracture network connectivity using percolation theory: Math. Geol., v. 27, no. 4, p. 467–483.

Berkowitz, B., and Adler, P. M., 1998, Stereological analysis of fracture network structure in geological formations: J. Geophys. Res., v. 103, no. B7, p. 15339–15360.

Black, J. H., 1994, Hydrogeology of fractured rocks, a question of uncertainty about geometry: Appl. Hydrogeol., no. 3/94, p. 56–70.

Bour, O., and Davy, P., 1998, On the connectivity of three-dimensional fault networks: Water Resour. Res., v. 34, no. 10, p. 2611–2622.

Chilès, J.-P., and de Marsily, G., 1993, Stochastic models of fracture systems and their use in flow and transport modeling, *in* Bear, J., Tsang, C. F., and de Marsily, G., eds., Flow and contaminant transport in fractured rock: Academic Press, San Diego, CA., p. 169–236.

Dershowitz, W. S., and Einstein, H. H., 1988, Characterizing rock joint geometry with joint system models: Rock Mech. Rock Eng., v. 21, no. 1, p. 21–51.

Dershowitz, W. S., and Herda, H. H., 1992, Interpretation of fracture spacing and intensity, *in* Tillerson, N., and Wawersik, W., Proceedings of the 33rd US Symposium on Rock Mechanics, Balkema, Rotterdam, The Netherlands, p. 757–766.

Ferguson, C. C., 1985, Spatial analysis of extension fracture systems, a process modeling approach: Math. Geol., v. 17, no. 4, p. 403–425.

Fouché, O., 1999, Caractérisation géologique et géométrique et modélisation 3D des réseaux de discontinuités d'un massif granitique (Charroux-Civray, France) reconnu par forages carottés: Doctoral Dissertation in Engineering Geology, Ecole nationale des Ponts et Chaussées, Ecole des Mines de Paris, Paris, France, 296 p.

Fouché, O., Cojean, R., and Arnould, M., 2001, Geological and geometrical characterization of natural fractures in a granitic formation from cored boreholes: Bull. Eng. Geol. Environ., v. 60, no. 3, p. 231–240.

Fouché, O., and Lacquement, F., 2001, Structural control on hydraulic connection through the Poitou basement (France) and the contact with its sedimentary cover, *in* Seiler, K.-P., and Wohnlich, S., eds., New approaches to characterising groundwater flow, Proceedings of the XXXI Congress of International Association of Hydrogeology, Munich, Germany, 10–14 September 2001, Balkema, Rotterdam, The Netherlands, supplement.

Fouché, O., and Meilliez, F., submitted for publication, Emplacement-Related Fracturing of a Plutonic Complex in a Hidden Variscan Segment (Poitou Strait, France): Terra Nova.

Fouché, O., Wright, H., Le Cléac'h, J.-M., and Pellenard, P., in press, Fabric control on strain and rupture of heterogeneous shale samples by using a non-conventional mechanical test: Appl. Clay Sci.

Gillespie, P. A., Howard, C. B., Walsh, J. J., and Watterson, J., 1993, Measurement and characterization of spatial distributions of fractures: Tectonophysics, v. 226, p. 113–141.

Gros, Y., and Genter, A., 1997, Évolution de la fracturation dans le socle de Seuil du Poitou (massif de Charroux—Civray, Vienne), caractérisation structurale et organisation spatiale multi-échelle, *in* Étude du massif de Charroux—Civray: Actes des journées scientifiques CNRS/ANDRA, Poitiers, France, 13–14 October 1997, p. 105–143.

Halbwachs, Y., Courrioux, G., Renaud, X., and Repusseau, P., 1996, Topological and geometric characterization of fault networks using 3D generalized maps: Math. Geol., v. 28, no. 5, p. 625–656.

Hudson, J. A., and Priest, S. D., 1983, Discontinuity frequency in rock masses: Int. J. Rock Mech. Min. Sci. Geomech. Abstr., v. 20, no. 2, p. 73–89.

Karcz, I., and Dickman, S. R., 1979, Determination of fracture intensity: Tectonophysics, v. 56, p. T1–T7.

Kulatilake, P. H. S. W., Wathugala, D. N., and Stephansson, O., 1993, Joint network modelling with a validation exercise in Stripa Mine, Sweden: Int. J. Rock Mech. Min. Sci. Geomech. Abstr., v. 30, no. 5, p. 503–526.

LaPointe, P. R., and Hudson, D. W., 1985, Characterization and interpretation of rock mass joint patterns: Geological Society of America Special Paper 199, 37 p.

Lebon, P., and Mouroux, B., 1999, Knowledge of the three french underground laboratory sites: Eng. Geol., v. 52, issue 3–4, p. 251–256.

Marrett, R., 1996, Aggregate properties of fracture populations: J. Struct. Geol., v. 18, no. 2/3, p. 169–178.

Martel, S. J., 1999, Analysis of fracture orientation data from boreholes: Environ. Eng. Geosci., v. V, no. 2, summer 1999, p. 213–233.

Mauldon, M., 1994, Intersection probabilities of impersistent joints: Int. J. Rock Mech. Min. Sci. Geomech. Abstr., v. 31, no. 2, p. 107–115.

Mauldon, M., and Mauldon, J. G., 1997, Fracture sampling on a cylinder: From scanlines to boreholes and tunnels: Rock Mech. Rock Eng., v. 30, no. 3, p. 129–144.

Meyer, T, Einstein, H. H., and Ivanova, V., 1999, Geologic stochastic modeling of fracture systems related to crustal faults, *in* Vouille, G., and Berest, P., eds., Proceedings of the 9th International Congress of Rock Mechanics, Ecole des Mines, Paris, France, Vol. 1, p. 493–497.

Priest, S. D., 1985, Hemispherical projection methods in rock mechanics: George Allen & Unwin, London, 124 p.

Pusch, R., 1998, Categorization of discontinuities for conceptual description of rock hosting repositories for hazardous waste: International workshop on computational methods in rock mechanics, Lund, Sweden: Eng. Geol., special issue, v. 49, no. 3–4, p. 177–183.

Renshaw, C. E., 1998, Sample bias and the scaling of hydraulic conductivity in fractured rock: Geophys. Res. Lett., v. 25, no. 1, p. 121–124.

Ross, S. M., 1983, Stochastic processes: Wiley, New York, 309 p.

Rouleau, A., and Gale, J. E., 1985, Statistical characterization of the fracture system in the Stripa granite, Sweden: Int. J. Rock Mech. Min. Sci. Geomech. Abstr., v. 22, no. 6, p. 353–367.

Santalo, L. A., 1976, Integral geometry and geometric probability: Addison-Wesley, Reading, Massachusetts, 434 p.

Starzec, P., and Andersson, J., 2002, Probabilistic predictions regarding key blocks using stochastic discrete fracture networks—example from a rock cavern in south-east Sweden: Bull. Eng. Geol. Environ., v. 61, no. 4, p. 363–378.

Terzaghi, R., 1965, Sources of error in joint surveys: Géotechnique, v. 15, no. 3, p. 287–304.

Vermilye, J. M., and Scholtz, C., 1995, Relation between vein length and aperture: J. Struct. Geol., no. 17, p. 423–434.

Warburton, P. M., 1980, A stereological interpretation of joint trace data: Int. J. Rock Mech. Min. Sci. Geomech. Abstr., v. 17, p. 181–190.

Wathugala, D. N., Kulatilake, P. H. S. W., and Stephansson, O., 1990, A general procedure to correct sampling bias on joint orientation using a vector approach: Comput. Geotechnics, v. 10, p. 1–31.

Weibel, E. R., 1980, Stereological methods, theoretical foundation: Academic Press, London, 340 p.

Xu, J., and Cojean, R., 1990, A numerical model for fluid flow in the block interface network of three dimensional rock block system, *in* Rossmanith, H. P., ed., Proceedings of the International Conference on Mechanics of Jointed and Faulted Rock, Vienna, Austria: Balkema, Rotterdam, The Netherlands, p. 627–633.

APPENDIX A: CORRECTION FOR MEAN ORIENTATION OF A FRACTURE SET AND SIMULATION

According to the assumption of independence between azimuth and plunge, and working in the borehole-based reference frame where the borehole axis is the z-axis, the apparent azimuth within a set remains unbiased whereas the apparent plunge is biased and must be weighted independently. This suggests to split the fracture pole-vector $\mathbf{V}$ (or the dip-vector) into two components: the azimuth-vector $\mathbf{V}_\alpha$ may be represented in the $(\mathbf{x};\mathbf{y})$ plane orthogonal to $\mathbf{z}$, and the plunge-vector $\mathbf{V}_\beta$ may be represented in the $(\mathbf{V}_\alpha;\mathbf{z})$ plane. The conversion of $\mathbf{V}$ to the geographic reference frame, if needed, may be done later using a rotation matrix.

For each set, treated independently, averaging the $\mathbf{V}_\alpha$'s directly provides the unbiased mean azimuth-vector, but we have to choose an adequate length for the counting interval of plunge values. Then, in each interval, we apply the frequency-dependent weighting based on Equations (1) and (2) to the $\mathbf{V}_\beta$'s, with θ the average apparent plunge in the interval: the weighted sum of all the $\mathbf{V}_\beta$'s provides the corrected mean plunge-vector $\overline{\mathbf{V}}_\beta$. The approximate dispersion of the $\mathbf{V}_\beta$'s with $\overline{\mathbf{V}}_\beta$ is computed from only the $\mathbf{V}_\beta$'s which do not lie between $\overline{\mathbf{V}}_\beta$ and the blind circle. Finally, knowing the corrected mean value and standard deviation, the distributions of the apparent α's and β's are selected via the Kolmogorov–Smirnov goodness-of-fit test, the most common being of normal or uniform type. The simulation of a set is performed in its borehole reference frame as a product sampling of the distribution fitted on $\mathbf{V}_\alpha$ and the distribution fitted on $\mathbf{V}_\beta$. The apparent α and β are converted into Cartesian coordinates. An example of a fracture set (no. 6 of Table 2) simulated according to this method is displayed in Figure A1.

APPENDIX B: SLOT SAMPLING PROBABILITY

This reduces to expressing the probability that a 2D Poisson segment is crosscut by the slot. To each segment i we associate the projected interval $[x_i - r_i \cos\beta_i;\ x_i + r_i \cos\beta_i]$ whose length is $2r_i \cos\beta_i$. We consider that all these intervals are included in $[0; L]$ since $\overline{r}_\alpha < L/2$. If $\mathbf{1}(\mathrm{K})$ denotes the indicator function of K, the proportion n_α/I_α of the projected intervals including the segment

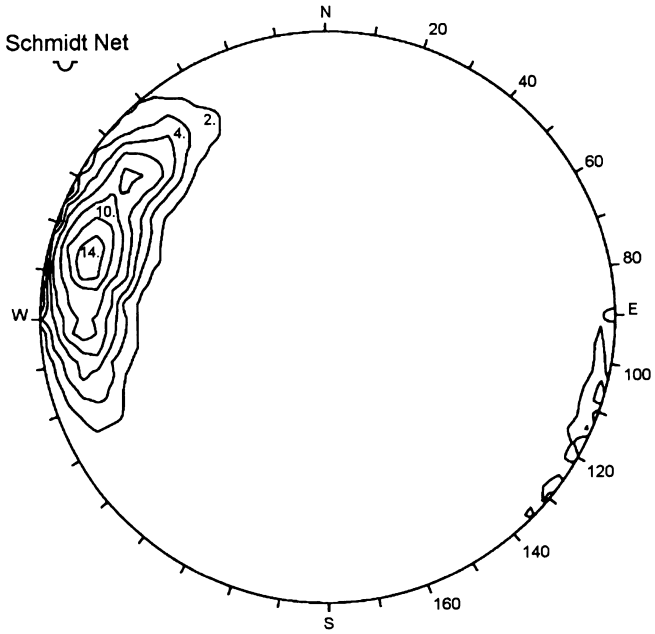

Figure A1. Distribution of fracture poles within a set model characterized by stochastic independence of azimuth and plunge. This model aims to represent set n°6 described in Table 2. A stochastic sample of this model is displayed in Figure 7(B) together with five other sets.

$[L/2-\varepsilon; L/2+\varepsilon]$ is

$$p = \frac{1}{I_\alpha} \cdot \sum_{i=1}^{I} \mathbf{1}([L/2-\varepsilon; L/2+\varepsilon] \subset [x_i - r_i \cos\beta_i; x_i + r_i \cos\beta_i])$$

By the strong law of large numbers, this proportion converges almost surely (a.s.) to

$$\mathbf{P}([L/2-\varepsilon; L/2+\varepsilon] \subset [X - R \cdot \cos B; X + R \cdot \cos B]) \quad \text{as} \quad I_\alpha \to \infty$$

Since

$$[L/2-\varepsilon; L/2+\varepsilon] \subset [x - r\cos\beta; x + r\cos\beta]$$
$$\Leftrightarrow x \in [L/2 + \varepsilon - r\cos\beta; L/2 - \varepsilon + r\cos\beta]$$

we obtain that the proportion p converges a.s. to

$$\mathbf{P}(X \in [L/2 + \varepsilon - R \cdot \cos B; L/2 - \varepsilon + R \cdot \cos B]) \quad \text{as} \quad I_\alpha \to \infty$$

where this probability may be expressed as

$$P = \int_r \int_\theta \mathbf{P}(x \in [L/2 + \varepsilon - r \cos\beta; L/2 - \varepsilon + r \cos\beta]) \cdot f(\beta) \cdot g(r) \cdot d\beta \cdot dr$$

A helpful theorem on Poisson processes (Ross, 1983) states that given I the number of events until time t, the I arrival times have the same distribution as the order statistics corresponding to I independent variables uniformly distributed on the interval $[0; t]$. In our case, under the condition that I_α events have occurred on the interval $[0; L]$, the I_α positions X_i are unordered independent random variables distributed uniformly on $[0; L]$. Therefore, on any interval $[a - \omega; b + \omega]$ included in $[0; L]$ where Ω is the random variable $R \cdot \cos B$, the variable X has a uniform distribution:

$$P = \int_r \int_\beta \frac{(b + \omega) - (a - \omega)}{L} \cdot f(\beta) \cdot g(r) \cdot d\beta \cdot dr$$

Since ε is very small compared to the expectation $\mathbf{E}(\Omega)$ it results that

$$P = \int_r \int_\beta \frac{2r \cos\beta - 2\varepsilon}{L} \cdot f(\beta) \cdot g(r) \cdot d\beta \cdot dr \approx \frac{2}{L} \cdot \int_\omega \omega \cdot f(\omega) \cdot d\omega = \frac{2\mathbf{E}(\Omega)}{L}$$

Since the random variables R and B are independent,

$$P \approx \frac{2}{L} \cdot \int_r r \cdot g(r) \cdot dr \cdot \int_\beta \cos\beta \cdot f(\beta) \cdot d\beta \tag{29}$$

Let us assume that I_α and n_α are so large that the following approximations of expectation by average are valid (it is further referred as A-E approximation):

$$\int_r r \cdot g(r) \cdot dr = \frac{1}{I_\alpha} \sum_{i=1}^{I_\alpha} r_i = \bar{r}_\alpha \tag{30}$$

$$\int_\beta \cos\beta \cdot f(\beta) \cdot d\beta = \frac{1}{n_\alpha} \sum_{i=1}^{n_\alpha} \cos\beta_i \quad \text{and}$$

$$\int_{\beta} \frac{1}{\cos\beta} \cdot f(\beta) \cdot d\beta = \frac{1}{n_\alpha} \sum_{i=1}^{n_\alpha} \frac{1}{\cos\beta_i} \tag{31}$$

Since for I_α large enough, the proportion n_α / I_α is approximately equal to P, it follows that

$$I_\alpha \approx \frac{n_\alpha}{P} \approx \left(\frac{L \cdot n_\alpha^2}{2\bar{r}_\alpha} \right) \Big/ \sum_{i=1}^{n_\alpha} \cos\beta_i \tag{32}$$